Published in final edited form as:
Integr Biol (Camb). 2013 March ; 5(3): 474–480. doi:10.1039/c3ib20259c.

Non-dimensional analysis of retinal microaneurysms: critical threshold for treatment

Elishai Ezra[a], **Eliezer Keinan**[a], **Yossi Mandel**[b], **Michael E. Boulton**[c], and **Yaakov Nahmias**[a,d]

Yaakov Nahmias: ynahmias@cs.huji.ac.il

[a]Center for Bioengineering, The Hebrew University of Jerusalem, Jerusalem, Israel

[b]Hansen Experimental Physics Laboratory, Stanford University, Stanford, California, USA

[c]Department of Anatomy and Cell Biology, University of Florida, Gainesville, Florida, USA

[d]Department of Cell and Developmental Biology, The Hebrew University of Jerusalem, Jerusalem, Israel

Abstract

Fluid dynamics play a fundamental role in the development of diabetic retinopathy, one of the leading causes of blindness in the Western world, affecting over 4 million people in the US alone. The disease is defined by microaneurysms, local expansions of capillaries that disturb the hemodynamic forces experienced by the endothelium leading to dysfunction, leakage and edema. Here we present a method to identify microaneurysms with a high risk of leakage based on a critical ratio of microaneurysm to vessel diameter. We derive this non-dimensional parameter from an analytical solution and generalize it using experimentally validated numerical methods. We show that this non-dimensional parameter defines the shear force experienced by endothelial cells, below which endothelial dysfunction is evident *in vivo*. Our results demonstrate the involvement of vWF in diabetic retinopathy, and explain a perceived disconnect between microaneurysm size and leakage. This method will allow experts to treat microaneurysms poising a high-risk of leakage, prior to edema, minimizing damage and saving vision.

Introduction

Microaneurysms are a dilation of microvasculature formed due to disruption of the internal elastic lamina.[1–3] This expansion disturbs the normal flow pattern, changing shear force and pressure along the vessel. Shear force plays a key role in promoting the differentiation and proliferation of endothelial cells.[4] Increasing evidence suggests that shear force plays a role in the evolution of cerebral aneurysms by promoting local proliferation of endothelial cells.[5,6] Boussel *et al.* showed a linear correlation between shear force and aneurysm dimensions that can result in rupture or thromboembolism.[5] A similar mechanism holds for *Charcot–Bouchard* microaneurysms, which present a major threat to a patient's life because of the risk of rupture, hemorrhage and stroke.[3] Retinal microaneurysms are a similar pathology and an early feature of diabetic retinopathy, one of the leading causes of blindness in the United States.[1,2] Diabetic retinopathy is responsible for 5% of the cases of blindness worldwide and up to 17% of the cases in the Western world. Retinal microaneurysms reduce vision due to local loss of endothelial barrier function, causing leakage and retinal edema. Localized leakage can be detected and treated using laser ablation slowing the progression of diabetic blindness.[7–9] The relationship between microaneurysms and leakage is unclear, as small microaneurysms can sometimes leak when large ones do not. In addition, leakage

Correspondence to: Yaakov Nahmias, ynahmias@cs.huji.ac.il.

can sometimes occur in the retinal 'background' where only capillaries are found. Understanding these phenomena and the role microaneurysms play in loss of vision could become an important tool for clinical diagnostics.

Attempts to characterize fluid behavior in complex geometries rely on analytical or numerical tools. For example, Tsangaris and Leiter[10] provided an analytical solution for flow in a channel with symmetrical sinusoidal disturbances. The solution is valid as long as the disturbance is small. On the other hand, Boussel *et al.* used numerical simulations of flow in varying geometries to compute shear force distributions as a function of local aneurysm wall displacement.[5] Such a numerical solution is valid for all conditions, but is computationally intensive and requires knowledge of exact geometries. An alternative approach to characterize the effect of complex geometries on fluid behavior is to use non-dimensional analysis to find a parameter that describes fluid behavior within a set of arbitrary conditions. Such a parameter could be used to rapidly calculate changes in fluid velocity, shear force, or fluid pressure due to microvessel expansion without the need for complex analytical or numerical solutions.

Here we demonstrate that changes in fluid velocity, shear force, and fluid pressure are dependent on a non-dimensional expansion parameter Δ which defines the ratio between main vessel and aneurysm diameters. The parameter Δ was derived from an analytical solution, valid for small disturbances, and numerically validated for varying geometries, fluid velocities and viscosities. Using a shear threshold for endothelial dysfunction, we calculated a critical expansion Δ_t above which leakage may occur. To validate our findings we obtained high-resolution confocal images of diabetic retinas, and observed that microaneurysms above our critical threshold demonstrate a dramatic, size-dependent increase in Von Willebrand factor (vWF) expression, a marker of endothelial dysfunction.[11] Our results demonstrate the previously unknown involvement of vWF in diabetic retinopathy, and explain a perceived disconnect between microaneurysm size and leakage. This method will allow experts to rapidly identify and treat microaneurysms that pose a high-risk of leakage, prior to edema, minimizing damage and saving vision.

Results

Analytical model

Newton's second law for fluids is formulated as the Navier–Stokes equations. The solution of these equations can be expressed as the stream function. A streamline is a virtual barrier, which no flow crosses, and the stream function is a mathematical expression that has a constant value on each streamline. The velocity distribution in a laminar flow is a partial derivative of the stream function. Tsangaris and Leiter provided an analytical solution of the stream function for a channel with small symmetrical sinusoidal disturbances:[10]

$$\psi=\zeta-\frac{\zeta^3}{3}+\varepsilon\cos\eta\left((A\sinh\zeta+B\zeta\cosh\zeta)-\zeta\left(1-\zeta^2\right)\right) \quad (1)$$

where ψ is the stream function, η is the normalized *y*-axis location, ranging from −1 to 1, ζ is the normalized *x*-axis location, ranging from 0 to 1, ε is the non-dimensional channel expansion (eqn (3); Fig. 1A), and *A* and *B* are calculated coefficients.

The derivation of the stream function in the *x*-axis distance variable (ζ) gives the perpendicular velocity component:

$$v=\varepsilon\cos\eta(A\sinh\zeta+B\zeta\cosh\zeta) \quad (2)$$

$$\varepsilon = \frac{R}{R+W} \quad (3)$$

where ε is the normalized velocity in the perpendicular direction, R is the disturbance radius and W is the undistorted channel width. The normalized velocity is converted to the real velocity with substitution of global parameters such as the channel velocity and the cavity dimensions.

Experimental validation of the numerical model

The analytical solution shown above is only valid for small disturbances ($R \ll W$). To gain a deeper understanding of the phenomenon we chose to expand it numerically. To validate the solution of the numerical model we tested its predictions experimentally by tracing the path of fluorescent beads in microchannels with varying velocities and geometries. Fig. 1D shows the stabilization distance of streamlines at velocities ranging from 0.01 to 0.001 m s^{-1} and radial disturbance diameters ranging from 50 to 125 μm. The experimental results showed an excellent correlation with numerical predictions ($R^2 = 0.98$). As could be expected, the stabilization distance increased with increasing flow rates and disturbance diameter. Interestingly, the similarities of this behavior across flow and size strongly suggest the presence of non-dimensional descriptors.

Dimensional analysis of fluid velocity

The analytical solution presented above suggests that fluid velocity is dependent on the non-dimensional expansion ε (eqn (3)). Fig. 2A plots the normalized tangential velocity as a function of non-dimensional expansion ε for both numerical and analytical results. As can be expected, the analytical and numerical results are in agreement only for small expansions where $R \ll W$ and the analytical solution is valid. Importantly, the numerical solutions show that the tangential velocity remains dependent on the non-dimensional expansion ε for an arbitrary set of velocities and perturbations, even for large disturbances and rapid flows where the analytical solution is no longer valid.

Dimensional analysis of shear force and pressure

Shear force plays an important role in hemodynamics. A drop in shear due to a local expansion of the vessel (aneurysm) can result in a loss of endothelial barrier function, leakage, and tissue damage. Fig. 2B shows shear force in the middle of the disturbance, one cell diameter from the wall, for varying Reynolds numbers as a function of non-dimensional expansion ε. The results show similar behavior for all Reynolds numbers, suggesting that the behavior depends only on ε. Indeed, when wall shear force is normalized to the average shear in the channel (Fig. 2C) it is solely dependent on the non-dimensional expansion ε at creeping flow (Re <1). Changes in pressure are dependent on friction losses that are related to the shear force, suggesting that similar behavior holds. The pressure in the border between the main channel and the middle of the disturbance was calculated and normalized to the pressure in the main channel. Fig. 2D shows that the normalized pressure is also dependent on the non-dimensional expansion ε for creeping flow (Re < 1). Small deviations from this behavior are seen for shear and pressure at Reynolds numbers of 8.5 and 85.

Dimensional limits of endothelial dysfunction in retinal microaneurysm

Retinal microaneurysms are local disturbances in the diameter of the blood vessels of the retina. Endothelial dysfunction in these microaneurysms can lead to leakage and retinal edema resulting in a progressive loss of vision. Recent work showed that endothelial dysfunction occurs when shear force drops below 0.4 Pa,[4] enabling us to calculate a critical non-dimensional expansion (ε) of 0.38 using Fig. 2C. Small blood vessels, such as

capillaries, venules, and arterioles exhibit a creeping flow placing them within the scope of our analysis (Table 1). Our analysis sets a critical aneurysm diameter of 15 μm for capillaries, 25 μm for venules and 104 μm for arterioles, above which endothelial dysfunction is predicted to occur. These results are intriguing as microaneurysms are thought to be larger than 40 μm.[9]

To test this hypothesis we obtained high-resolution confocal images of human diabetic retinas and quantified microaneurysm size distribution (Fig. 3A). Interestingly, the mean microaneurysm diameter was 34 ±16 μm, with 60% of them smaller than 40 μm in diameter (Fig. 3B). To find whether endothelial dysfunction occurs above our threshold, we quantified vWF staining as a function of our non-dimensional expansion (Fig. 3C). The results are presented as average fluorescence units per unit area, normalized to background. Distribution of staining in normal microvasculature and the critical expansion parameter are marked for reference. Remarkably, while vWF expression in microaneurysms below our threshold was not significantly different from that in the surrounding micro-vasculature ($p = 0.076$), it was 60 ±10% lower than in microaneurysms above our threshold ($p = 2 \times 10^{-11}$). In fact, all microaneurysms showed a strong positive correlation between vWF expression and Δ ($R^2 = 0.89$), similar behavior was not observed in normal vessels. In contrast to the high correlation between vWF and our non-dimensional parameters (Fig. 3D), there was only a weak correlation between vWF staining and aneurysm size ($R^2 = 0.59$) (Fig. 3E). In fact, one can easily identify large microaneurysms that do not pose a risk, and smaller ones that do. Interestingly, microaneurysms smaller than 20–30 μm in diameter would not be identified in standard angiography and would appear as background retinal leakage. These results strongly suggest that both our critical expansion parameter and vWF staining can be used to predict which microaneurysm presents higher risk of leakage.[12,13]

Discussion

Diabetic retinopathy is one of the leading causes of blindness in the Western world, with associated medical costs of over $1 billion per year. With the growing prevalence of diabetes, these numbers are expected to double within the next few years. Retinal microaneurysms are the earliest sign of diabetic retinopathy, caused by the local expansion of capillaries in the retina. The exact mechanism of microaneurysm formation and the cause of leakage are not clearly understood. The potential role in pericyte loss, intraluminal pressure and smooth muscle cell loss have been implicated as the cause for microaneurysm formation.[14–17] The changing vessel geometry affects the hemodynamic forces experienced by the endothelial lining of the capillaries, leading to endothelial dysfunction, causing leakage, and retinal edema. During the early stages of the disease, vessel leakage can be treated using laser photo-coagulation to prevent further deterioration,[6] but as of now, there is no way to classify whether a microaneurysm poses a significant or a benign risk.

Our approach has been to gain a critical understanding of the fluid dynamics of the problem, which will enable us to predict the risk associated with the diseased morphology. However, analytical solutions of Navier–Stokes equations exist only for restricted conditions, while numerical simulations can only be performed on one set of initial and boundary conditions at a time. Uncovering non-dimensional behavior is an alternative approach,[18] which allows for rapid calculation of critical properties. We identified the non-dimensional expansion parameter Δ in the analytical solution reported by Tsangaris and Leiter which is restricted to small axisymmetric sinusoidal disturbance in creeping[19] and non-creeping flow.[10] Follow up work extended this solution to channel distortions of any geometry, while dependence on Δ remained,[20,21] suggesting that the behavior is more general. Here we used an experimentally validated numerical simulation to show that normalized tangential velocity, shear force, and pressure drop depend on the non-dimensional expansion Δ for arbitrary

viscosity and fluid velocity as long as the flow is creeping (Re < 1). At higher velocities, this dependency breaks down. For creeping flow we can define:

$$\frac{\tau_d}{\tau_{av}} = 60.85e^{-15.92\varepsilon} \quad (4)$$

where τ_d is the shear force at one cell diameter (10 μm) from the wall at the center of the disturbance and τ_{av} is the average shear force in the channel.

Several groups have studied the role of shear force in microaneurysm dysfunction. Boussel *et al.* used numerical simulation to show a correlation between shear force and retinal microaneurysm growth.[5] More recently, Cucullo *et al.* showed that shear forces above 0.4 Pa were required to establish barrier function of brain microvascular endothelial cells, based on protein, gene, and functional studies.[4] This value is significantly lower than the normal shear stress reported for retinal arterioles or venules.[22] Our hypothesis was that retinal microvascular endothelial cells behave similarly allowing us to calculate the critical non-dimensional expansion for capillaries (Re = 0.002), venules (Re = 0.01), and arterioles (Re = 0.7). Table 1 shows our prediction, with a critical expansion (ε) of 0.38 for capillaries and venules, and 0.52 for arterioles. These predictions could now be tested *in vivo*.

While endothelial dysfunction is difficult to measure *in vivo*, several groups suggested that the endothelial-synthesized Von Willebrand factor (vWF) could serve as a nonspecific marker of endothelial dysfunction. Indeed, elevated plasma levels of vWF precede the development of nephropathy in diabetic patients and strongly correlate with vascular events. However, plasma levels of vWF were not correlated with progression of diabetic retinopathy perhaps due to the small size of the retina.[23,24] Here we demonstrate that a careful analysis of vWF in diabetic retina blood vessels shows a marked increase in expression as a function of our non-dimensional expansion parameter (Fig. 3D) but not as a function of microaneurysm size (Fig. 3E). These results are in good agreement with prior studies that found no correlation between aneurysm size and leakage.

Interestingly, there are only a few reports on the association between shear force and vWF expression. Galbusera and colleagues suggested that vWF is retained by the endothelium when shear forces are low.[25] Our results identify a highly significant correlation for microaneurysm above our threshold with vWF staining *in vivo* ($p = 2 \times 10^{-11}$), suggesting a critical threshold for endothelial dysfunction. Taken together, the results suggest that both our critical expansion parameter, and vWF staining can be used to predict which microaneurysm presents a higher risk of leakage.

The rapid advance of optics over the last decade permits the high-resolution imaging of retinas *in vivo* with and without the use of fluorescent functional markers, such as vWF. The current treatment strategy for diabetic retinal edema has been dramatically changed since the introduction of anti-VEGF injections.[26] Large leaking microaneurysms are generally treated by focal application of laser ablation, while a diffuse “retinal background” leakage is treated in a grid pattern or by early injection of anti-VEGF agents. Our results suggest that some cases of diffuse leakage are caused by small microaneurysms. We show that even an aneurysm with a size of 15 μm can potentially develop endothelial dysfunction (Table 1). While current imaging techniques cannot detect this small aneurysm,[27] emerging ophthalmic diagnostics methods such as OCT can reach a resolution of 2 μm.[28,29]

In summary our results show that the expansion parameter ε and vWF staining can be used to predict the microaneurysm risk profile and may indicate early treatment options. We note that our analysis holds for brain *Charcot–Bouchard* microaneurysms as well. Brain microaneurysms pose a significant risk of rupture causing hemorrhages and stroke.

Materials and methods

Numerical modeling

Numerical simulations were performed using COMSOL multi-physics simulation platform v3.5A with a direct (PARADISO) linear system solver and an extra fine mesh. The fluid density was defined as 1×10^3 kg m^{-3}, with a dynamic viscosity of 1×10^{-3} Pa s. To experimentally validate the numerical solution we predicted the stabilization of flow going past a cavity, and compared it to measurements of stabilization in microfabricated channels of the same geometry and flow. We defined the stabilization distance as the location with a perpendicular velocity component lower than 0.01 cm s^{-1}.

Experimental validation of the numerical model

Poly(dimethyl)siloxane (PDMS) was purchased from Dow Corning (Midland, MI). SU8-2050 was purchased from Microchem (Newton, MA). Fluorescent beads and Pluronics F68 were purchased from Sigma Aldrich (Rehovot, Israel). Microfluidic devices were fabricated by soft lithography at the Hervey Krueger Center of Nanoscience and Nanotechnology at the Hebrew University of Jerusalem. Briefly, molds were fabricated by photolithography of SU8 on silicon. Channels were replica molded in PDMS and bonded to glass using oxygen plasma bonding as previously described.[30,31] The channels were 100 μm high with a width of 3000 μm. Six circular disturbances ranging from 25 to 200 μm emanated from the main channel. Micro-fabricated channels were coated with Pluronic F68 to prevent non-specific binding of beads. Suspensions of 2×10^6 beads per mL were perfused at velocities ranging from 0.001 to 0.1 m s^{-1}. Particle trajectories were captured on a Zeiss Axiovert Z1 using high-resolution fluorescence microscopy. To quantify stabilization distance we calculated the perpendicular velocity by dividing the shift of the particle in the perpendicular direction by the time it takes to traverse the cavity. The time to traverse the cavity was calculated from the fluid velocity, accounting for the 2 orders of magnitude difference between the perpendicular and tangential components.

Preparation and imaging of diabetic retinas

Postmortem donor eyes of diabetic patients with early retinopathy characterized by the presence of microaneurysms were obtained from the National Disease Research Interchange (Philadelphia, USA) and processed as previously described.[32] All human eyes used in this study were obtained from the National Disease Research Interchange, Philadelphia, PA, and all experiments were performed in compliance with the laws and institutional guidelines at the University of Manchester, Manchester, UK, where the tissue was examined, and with appropriate institutional approval for the experiments.

Briefly, tissue was fixed within 24 hour postmortem with 10% neutral buffered formalin. The anterior segment and vitreous were removed and a rectangular incision of 250 mm^2 including the optic nerve head, macula and temporal vascular arcades. The retina was gently detached from the underlying RPE, washed with PBS and incubated with chymotrypsin to expose epitopes. The tissue was permeablised using 0.2% Triton X100 for 1 h. Tissues were blocked in 20% normal goat serum and incubated overnight with a 1 : 50 dilution of rabbit anti-human vWF from Dako (Carpinteria, CA). Following a 3 hour wash in PBS, retinas were incubated overnight with 1 : 50 dilution of goat anti-rabbit FITC from Sigma (St. Louis, MO), washed and mounted. Retinas were examined from the vitreous surface using a Biorad MRC 600 confocal laser scanning attachment mounted on a Zeiss Axiovert microscope using a 25 mW argon laser (Ion Laser Technology). Maximum projection images were analyzed using the Image J software (NIH) to quantify microaneurysm geometry and average vWF intensity.

Conclusions

We discovered a non-dimensional parameter that defines the behavior of fluids in complex geometries. This parameter allows us to rapidly quantify physical parameters, such as shear flow, under arbitrary conditions. We applied our non-dimensional parameters to diabetic retinopathy, one of the leading causes of blindness in the Western world, with associated medical costs of over $1 billion per year. We defined a critical geometric ratio above which endothelial dysfunction is evident *in vitro*, and validated our findings in high-resolution confocal images of retinas of diabetic patients.

Our results explain the observed disconnect between microaneurysm size and its risk of leakage, and provide simple ways to assess this risk. Moreover, we identified the Von Willebrand factor (vWF) as a marker for the microaneurysm risk in retinopathy.

References

1. Crawford TN, Alfaro DV, Kerrison JB, Jablon EP. Curr Diabetes Rev. 2009; 5(1):8–13. [PubMed: 19199892]
2. Curtis TM, Gardiner TA, Stitt AW. Eye. 2009; 23(7):1496–1508. [PubMed: 19444297]
3. Kohner EM, Stratton IM, Aldington SJ, Turner RC, Matthews DR. Diabetologia. 1999; 42(9):1107–1112. [PubMed: 10447523]
4. Cucullo L, Hossain M, Puvenna V, Marchi N, Janigro D. BMC Neurosci. 2011; 12:40. [PubMed: 21569296]
5. Boussel L, Rayz V, McCulloch C, Martin A, Acevedo-Bolton G, Lawton M, Higashida R, Smith WS, Young WL, Saloner D. Stroke. 2008; 39(11):2997–3002. [PubMed: 18688012]
6. Sierra C, Coca A, Schiffrin EL. Curr Hypertens Rep. 2011; 13(3):200–207. [PubMed: 21331606]
7. Browning DJ, Altaweel MM, Bressler NM, Bressler SB, Scott IU. Am J Ophthalmol. 2008; 146(5):649–655. [PubMed: 18774122]
8. Bindley CD, Wallow HL. Retina. 1988; 8(4):261–269. [PubMed: 3231918]
9. Wang H, Chhablani J, Freeman WR, Chan CK, Kozak I, Bartsch DU, Cheng L. Am J Ophthalmol. 2012; 153(5):861–867. [PubMed: 22300473]
10. Tsangaris S, Leiter E. Proc 1st Int Conf Mech Med & Biol. 1978:289–292.
11. Sowers, JR. Contemporary Endocrinology: Endocrinology of the Vasculature. Humana Press; Totowa, NJ: 1996.
12. Hollestelle MJ, Loots CM, Squizzato A, Renne T, Bouma BJ, de Groot PG, Lenting PJ, Meijers JC, Gerdes VE. J Thromb Haemostasis. 2011; 9(5):953–958. [PubMed: 21352469]
13. Murata M, Fukuyama M, Satoh K, Fujimura Y, Yoshioka A, Takahashi H, Handa M, Kawai Y, Watanabe K, Ikeda Y. J Clin Invest. 1993; 92(3):1555–1558. [PubMed: 8376606]
14. Speiser P, Gittelsohn AM, Patz A. Arch Ophthalmol. 1968; 80(3):332–337. [PubMed: 4174771]
15. Gardiner TA, Archer DB, Curtis TM, Stitt AW. Microcirculation. 2007; 14(1):25–38. [PubMed: 17365659]
16. Stitt AW, Gardiner TA, Archer DB. Br J Ophthalmol. 1995; 79(4):362–367. [PubMed: 7742285]
17. Gardiner TA, Stitt AW, Anderson HR, Archer DB. Br J Ophthalmol. 1994; 78(1):54–60. [PubMed: 8110701]
18. Nahmias YK, Gao BZ, Odde DJ. Appl Opt. 2004; 43(20):3999–4006. [PubMed: 15285089]
19. Tsangaris S, Leiter E. J Eng Math. 1984; 18(2):89–103.
20. Usha KHR, Amaranath T, Nigam R. Fluid Dyn Res. 1989; 5:83–89.
21. Zhou H, Martinuzzi RJ, Khayat RE, Straatman AG, Abu-Ramadan E. Phys Fluids. 2003; 15(10):3114–3133.
22. Nagaoka TA, Akitoshi Y. Invest Ophthalmol Visual Sci. 2006; 47(3):1113–1119. [PubMed: 16505049]

23. Boeri D, Cagliero E, Podesta F, Lorenzi M. Invest Ophthalmol Visual Sci. 1994; 35(2):600–607. [PubMed: 8113010]
24. Feng D, Bursell SE, Clermont AC, Lipinska I, Aiello LP, Laffel L, King GL, Tofler GH. Diabetes Care. 2000; 23(11):1694–1698. [PubMed: 11092294]
25. Galbusera M, Zoja C, Donadelli R, Paris S, Morigi M, Benigni A, Figliuzzi M, Remuzzi G, Remuzzi A. Blood. 1997; 90(4):1558–1564. [PubMed: 9269774]
26. Aiello LP, Beck RW, Bressler NM, Browning DJ, Chalam KV, Davis M, Ferris FL, Glassman AR, Maturi RK, Stockdale CR, Topping TM. Diabetic Retinopathy Clinical Research Network, Writing Committee. Ophthalmology. 2011; 118(12):e5–14. [PubMed: 22136692]
27. Keane PA, Sadda SR. Eye. 2010; 24(3):422–427. [PubMed: 20010789]
28. Takayama K, Ooto S, Hangai M, Arakawa N, Oshima S, Shibata N, Hanebuchi M, Inoue T, Yoshimura N. PLoS One. 2012; 7(3)
29. Rossi EA, Chung M, Dubra A, Hunter JJ, Merigan WH, Williams DR. Eye. 2011; 25(3):301–308. [PubMed: 21390064]
30. Whitesides GM, Stroock AD. Phys Today. 2001; 54(6):42–48.
31. Ng JM, Gitlin I, Stroock AD, Whitesides GM. Electrophoresis. 2002; 23(20):3461–3473. [PubMed: 12412113]
32. Moore J, Bagley S, Ireland G, McLeod D, Boulton ME. J Anat. 1999; 194(1):89–100. [PubMed: 10227670]
33. Talbot L, Berger SA. Am J Sci. 1974; 62:671–682.

Insight, innovation, integration

We define a critical geometric ratio above which endothelial dysfunction is evident *in vitro*, and validate our findings in high-resolution confocal images of retinas of diabetic patients. Our analysis identifies critical thresholds for microaneurysms leakage in capillaries, venules, and arterioles. These thresholds offer opportunities for preemptive treatment using laser photocoagulation to stop leakage from occurring, rather than reactive photocoagulation used nowadays to stop the progression of leakage once it occurred. Moreover, we show that Von Willebrand factor (vWF) expression *in vivo* is dependent on microaneurysm risk. We open the route for vWF targeted therapy or clinical detection: a simple vWF antibody can be used to localize fluorescein angiography to risky regions in the retina.

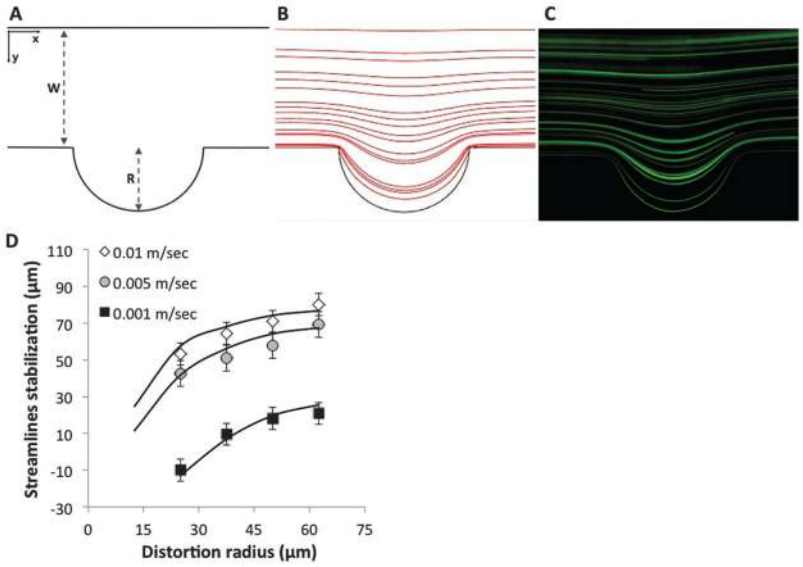

Fig. 1.

Experimental validation of the numerical model. (A) Schematic of channel and cavity. (B) Numerical streamline results obtained using COMSOL. (C) Experimental tracing of streamlines using long exposure capture of fluorescent beads. (D) Streamlines stabilization distance as a function of the cavity radius for 0.01 m s^{-1}, 0.005 m s^{-1} and 0.001 m s^{-1}. Numerical simulations (lines) are compared to experimental measurements (markers) showing excellent correspondence (R^2 = 0.98).

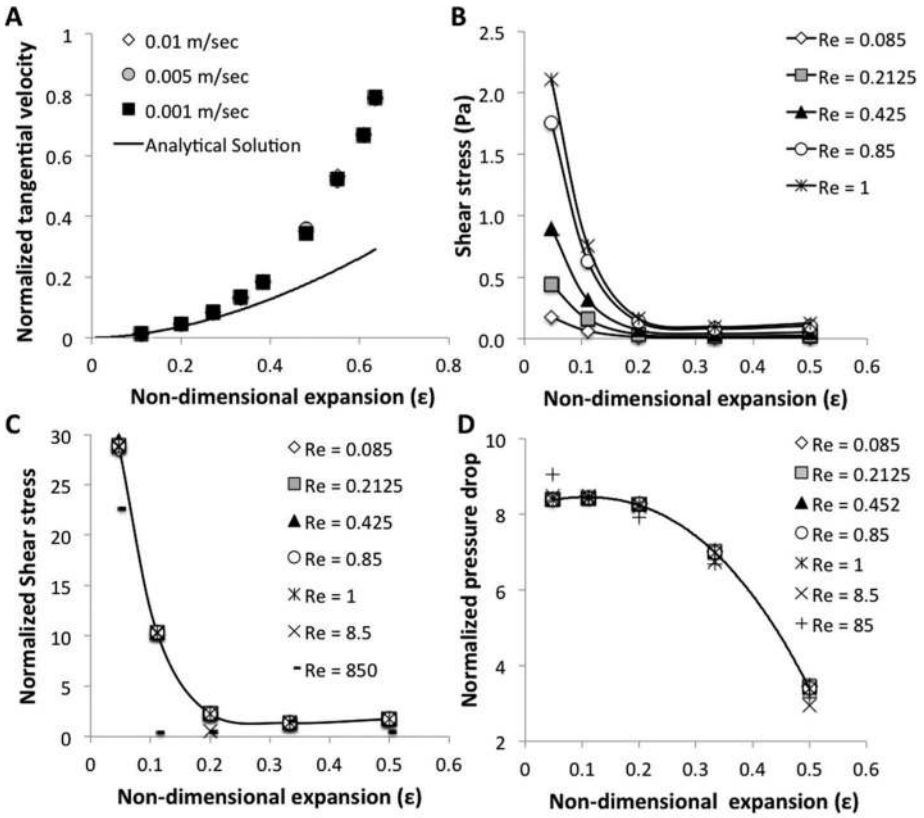

Fig. 2.

Non-dimensional analysis of fluid dynamics in aneurysm. (A) Normalized tangential velocity (*y*-axis divided by *x*-axis velocity) at the center of the cavity as a function of non-dimensional expansion parameter . Analytical solution (line) agrees with numerical simulation (markers) for small cavities. (B) Shear force 10 m from the channel wall at the center of the cavity as a function of the non-dimensional expansion parameter . Data were derived from numerical simulation for five flow regimes characterized by different Reynolds numbers. (C) Normalized shear force as a function of the non-dimensional expansion parameter . Shear force was normalized to the average shear in the channel. Data show that the normalized shear force is solely dependent on for Re < 1. (D) Normalized pressure drop in the middle of the cavity as a function of the non-dimensional expansion parameter . Pressure drop was calculated as the pressure difference between the middle of the undisturbed channel and the middle of the disturbance. The pressure drop was normalized to the Reynolds number. Data show that the normalized pressure drop is solely dependent on for Re < 1.

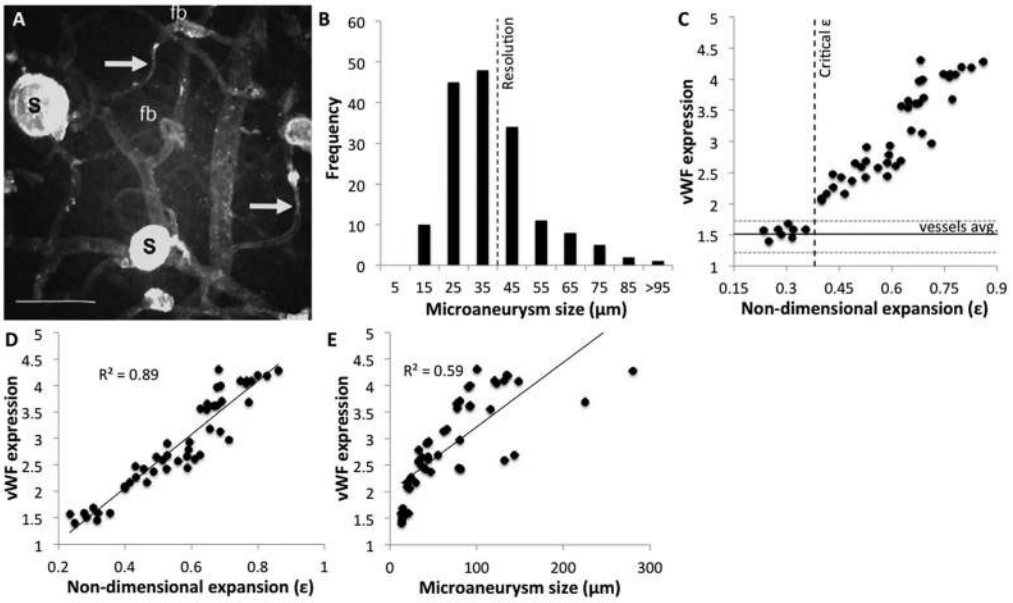

Fig. 3.

Evaluation of endothelial dysfunction in diabetic retinas. (A) Confocal maximum projection image of human diabetic retinas stained for vWF. Microaneurysms range from saccular (S) that stain strongly to vWF to focal bulges (fb). Bar = 100 μm. Image adapted from ref. 32. (B) Histogram of microaneurysm size distribution in the human diabetic retina. Microaneurysms were thought to be bigger than 40 μm, possibly due to limits of standard angiography equipment. (C) Quantification of vWF staining as a function of non-dimensional expansion ε. Fluorescence was averaged per unit area of aneurysm and normalized to background values. Microaneurysms below our threshold exhibit vWF expression similar to that of normal vessels ($p = 0.076$) while those above it showed a significantly higher expression ($p = 2 \times 10^{-11}$). (D) Microaneurysms showing a strong positive correlation between vWF expression and non-dimensional expansion ε ($R^2 = 0.89$). (E) The correlation between microaneurysm diameter and vWF expression is weak ($R^2 = 0.59$), explaining prevalent thoughts in the field.

Table 1

Calculated values for critical microaneurysms width in different blood vessels[33]

Vessels	Diameter (μm)	Velocity (m s^{-1})	Re	Average shear (Pa)	Critical shear (Pa)	Critical epsilon	Critical aneurysm width (μm)
Capillary	10	0.001	0.002	2.8	0.4	0.38	15
Venule	20	0.002	0.01	2.8	0.4	0.38	25
Arteriole	50	0.05	0.7	28	0.4	0.52	104
Vein	500	0.1	140	5.6	0.4	—	—
Artery	400	0.45	500	31.5	0.4	—	—